Hindawi Publishing Corporation
Science and Technology of Nuclear Installations
Volume 2008, Article ID 265430, 18 pages
doi:10.1155/2008/265430

Review Article

A Critical Review of the Recent Improvements in Minimizing Nuclear Waste by Innovative Gas-Cooled Reactors

E. Bomboni,[1] N. Cerullo,[1,2] G. Lomonaco,[1,3] and V. Romanello[1,4]

[1] *DIMNP, University of Pisa, CIRTEN, Via Diotisalvi 2, 56126 Pisa, Italy*
[2] *DIPTEM, University of Genovfa, Via all'Opera Pia 15/a, 16145 Genova, Italy*
[3] *Department of Energetics, University of Pisa, Via Diotisalvi 2, 56126 Pisa, Italy*
[4] *DII, University of Salento, Via per Arnesano, 73100 Lecce, Italy*

Correspondence should be addressed to N. Cerullo, cerullo@docenti.ing.unipi.it

Received 30 May 2007; Accepted 12 March 2008

Recommended by Nikola Cavlina

This paper presents a critical review of the recent improvements in minimizing nuclear waste in terms of quantities, long-term activities, and radiotoxicities by innovative GCRs, with particular emphasis to the results obtained at the University of Pisa. Regarding these last items, in the frame of some EU projects (GCFR, PUMA, and RAPHAEL), we analyzed symbiotic fuel cycles coupling current LWRs with HTRs, finally closing the cycle by GCFRs. Particularly, we analyzed fertile-free and Pu-Th-based fuel in HTR: we improved plutonium exploitation also by optimizing Pu/Th ratios in the fuel loaded in an HTR. Then, we chose GCFRs to burn residual MA. We have started the calculations on simplified models, but we ended them using more "realistic" models of the reactors. In addition, we have added the GCFR multiple recycling option using k_{eff} calculations for all the reactors. As a conclusion, we can state that, coupling HTR with GCFR, the geological disposal issues concerning high-level radiotoxicity of MA can be considerably reduced.

1. INTRODUCTION

Nowadays nuclear power is the only greenhouse-free source that can face the always increasing worldwide energy demand. The LWR technology (at present the most widespread technology) is secure and well-proven: its major "real" drawback is probably the scarce exploitation of uranium resource and the consequently "large" production of waste. In fact, annually a 1000-MW_e PWR produces about 30 tons of spent nuclear fuel (burnup around 30 GWD/tU) with the following average composition:

(i) 94% U^{238};
(ii) 1% U^{235} (please remember that natural uranium contains 0.7% of U^{235});
(iii) 1% Pu;
(iv) 0.1% MA (Np, Am and Cm);
(v) 3 ÷ 4% FP.

Considering the actual reprocessing technology, this quantity of SNF contains about 1200 kg of "waste" (i.e., FP + MA): such a vitrified waste occupies about 20 m^3, which correspond to the 0.002% of the total amount of domestic waste in UK, for instance [1].

On the other hand, it is a relatively small quantity of waste if compared with the conventional energy sources: a 1000-MW_e coal-fired power plant discharges annually $6 \cdot 10^6$ tons of CO_2, $2 \cdot 10^5$ tons of ashes, and $2 \cdot 10^5$ tons of SO_2 [2], that means a volume which is roughly $1 \cdot 6 \cdot 10^8$ times higher than that of vitrified nuclear waste. (In fact, at STP, $6 \cdot 10^6$ tons of CO_2 occupies $3 \cdot 10^9$ m^3, $2 \cdot 10^5$ tons of SO_2 occupies $7 \cdot 10^7$ m^3, and $2 \cdot 10^5$ tons of ashes (with a mean density of 1500 kg/m^3) occupies $1.33 \cdot 10^5$ m^3.) The main issue for the nuclear power opponents is that the spent fuel radiotoxicity takes more than 100000 years to reach the same amount of radiotoxicity as that of the uranium ore from which it descends. This long time is mainly due to Pu, but also if all the Pu would be transmuted, the time to reach the level of mine (LOM) would still be around some tens of thousand years because of the presence of the MAs.

However, if all the actinides were fissioned directly or indirectly (by conversion fertile-to-fissile), the "real"

remaining waste should be constituted by FP, that have a relatively short lifetime (not more than hundreds of years). Today Pu from SNF is partially recovered: France, UK, Japan, Russia, China, and India reprocess their spent fuel in order to fabricate new MOX fuel elements, while other countries, as USA and Sweden, adopt the OTTO cycle.

From a global point of view [3], 16% of the world energy demand is covered by nuclear power that supplies 350 GW_e, roughly equally subdivided under USA, Europe, and the rest of the world. These plants produce 10500 tHM/year of spent fuel, of which 3900 tHM/year are reprocessed. As already remembered, reprocessing plants recover U and Pu only, while MA are treated with FP as waste. Of this Pu (recovered form LWRs), only 25% is consumed in thermal reactors, while 10% is converted in MA. MOX fuel can be reprocessed not more than 2 times in order to manufacture new LWR MOX fuel (Pu isotopic vector becomes more and more poor in fissile nuclides, while many higher Pu isotopes and MA are poisons in the thermal spectrum) and its radiotoxicity increases because of Cm^{244} buildup [3].

Thus, it was clear since the beginning of nuclear age that different kind of reactor would be necessary in order to increase the availability of nuclear fuel. Researches on fast reactor technology started in the past in order to multiply by 50 the availability of nuclear fuel resources. According to the goals of sustainability, economics, and proliferation resistance of the Generation IV Initiative [4], all the HMs have to be seen as resource. To realize the so-called *full actinide recycle* or *integral fuel cycle* (i.e., a self-sustaining fuel cycle in which the feed is constituted by fertile material only), one improves 180 times the uranium resources exploitation than a *once-through* LWR cycle [5]. Please remember that using a closed fuel cycle, the uranium resources would be sufficient for around 2500 years at the actual consumption rate (considering only the "identified resources," that are only a fraction of the total worldwide uranium availability) [6].

The activity performed at the University of Pisa fits into this frame. From many years, the DIMNP group is studying gas-cooled reactors, which have been largely recovered by Gen-IV both thermal and fast (two of the six concepts proposed are gas-cooled reactors). They seem to have the capability to reach the Gen-IV goals thanks to their unique characteristics.

In this frame, it appears useful to analyze the impact on the entire fuel cycle of the symbiosis of LWR, HTR, and GCFR.

2. TRANSMUTATION PHYSICS

2.1. Theory

The term "transmutation" is applied to all the nuclear reactions which transform a nuclide into another nuclide. In nuclear reactors, transmutation happens by way of (n,c), (n,f), and $(n,2n)$ reactions typically. It is clear that the probability of transmutation for a nuclide is strictly linked to its effective cross-sections for (n,c), (n,f), $(n,2n)$ reactions in the considered core. Moreover, the transmutation rate depends obviously also from the neutron flux intensity. Let us call to mind some useful parameters in transmutation studies [7]. The neutron spectrum is defined as

$$\chi(\vec{r},E,t) = \frac{\varphi(\vec{r},E,t)}{\varphi(\vec{r},t)}, \tag{1}$$

where φ is the neutron flux, while the effective cross-section of the nuclide n for the reaction x is expressed by

$$\overline{\sigma}_{n,x}(\vec{r},t) = \int_{0.001\,\mathrm{eV}}^{10\,\mathrm{MeV}} \sigma_{n,x}(E)\chi(\vec{r},E,t)dE. \tag{2}$$

The upper integration limit depends from the fission spectrum (typical of a given nuclide); while the lower limit considers that at the reactor temperature, the neutron energy is higher than 0.001 eV (in an LWR the mean energy of the thermal neutrons is about 0.04 eV, e.g.).

The transmutation rate for a nuclide i is determined by Bateman's equations:

$$\begin{aligned}\frac{d}{dt}N_i(\vec{r},t) = &-\lambda_i N_i(\vec{r},t)\\ &-(\overline{\sigma}_{i,a}+\overline{\sigma}_{i,(n,2n)}+\cdots)N_i(\vec{r},t)\varphi(\vec{r},t)\\ &+\overline{\sigma}_{i-1,c}N_{i-1}(\vec{r},t)\varphi(\vec{r},t)+\overline{\sigma}_{i+1,(n,2n)}N_{i+1}(\vec{r},t)\varphi(\vec{r},t)\\ &+\sum_k N_k(\vec{r},t)\lambda_{k\to i}.\end{aligned} \tag{3}$$

Let us name $\overline{\sigma}_{i,a}+\overline{\sigma}_{i,(n,2n)}+\overline{\sigma}_{i,(n,3n)}+\cdots$ as $\overline{\sigma}_{i,t}$, effective transmutation cross-section of the nuclide i. The previous equations show that destruction rate is as high as follows.

(1) The effective transmutation cross-section of the nuclide i is high.

(2) The effective transmutation cross-sections of the precursory nuclides is small or, if it is high, its most important term is the fission cross-section.

(3) The fluence is high (i.e., the intensity of the neutron flux is high or the irradiation time is long).

(4) The decay constant of the nuclide i is high while the ones of the precursors are small.

The (n,xn) cross-sections of the actinides are not so important if compared with the capture or fission cross-sections, so we can neglect them in transmutation analysis. Similarly, the decay constants are small if compared with the transmutation rates. Then, we can use the following simplified equations:

$$\frac{d}{dt}N_i(\vec{r},t) = -\overline{\sigma}_{i,a}N_i(\vec{r},t)\varphi(\vec{r},t)+\overline{\sigma}_{i-1,c}N_{i-1}(\vec{r},t)\varphi(\vec{r},t). \tag{4}$$

In order to reduce the long-term radiotoxicity of the SNF, the best transmutation way is fission (direct, if the nuclide is fissile, or indirect, by way of conversion from fertile to fissile). In fact, capture reactions (also followed by decay) cause the buildup of other very radiotoxic actinides, while fissions produce elements with shorter (except few cases) half-lives. Please note that the effective cross-sections are obtained by weighting over the neutron spectrum.

2.2. Thermal versus fast spectrum

As showed by the previous equations, the energy distribution of the neutrons is a very important parameter from the transmutation point of view. Regarding HM, their typical absorption cross-section, as known, can be subdivided into three main regions as follows:

(1) thermal range, with an approximately $1/v$ trend (roughly up to 0.625 eV); in this region, the fission cross-section is larger than the capture cross-section only for the fissile nuclides;

(2) resonance region (between 0.625 eV and 100 keV);

(3) fast region (above 100 keV), where the fission and capture cross-section are similar, around 1 barn; particularly, all the HM nuclides are fissile above 1 MeV (threshold).

Although the fission spectrum is fast (the mean energy is around 2 MeV, while the most probably energy is about 1 MeV), interactions between neutrons and the materials of a fast reactor (i.e., inelastic and elastic scatterings) cut off the mean energy to about $100 \div 200$ keV. So, the fission of fertile nuclides by neutrons above the threshold is rare ($\varepsilon \approx 1.15 \div 1.20$ in fast reactors [8]).

Nevertheless, in order to transmute the HM, a fast spectrum is better than a thermal one because of the following.

(i) The higher fluence due to the higher neutron flux intensity (in fast spectrum the effective fission cross-section is lower, so that an higher flux intensity is requested to produce the same fission power) increases the HM consumption.

(ii) In fast spectrum, the $\alpha = \sigma_c/\sigma_f$ ratio is smaller than in thermal for many actinides.

(iii) The neutron production $\nu\sigma_f$ is higher, so that there is an excess of neutrons which are available to transmute nuclides.

These considerations can be summarized by a "reactivity parameter" (RP) defined [8] as

$$\mathrm{RP} = \sigma_f(\nu - 1 - \alpha). \tag{5}$$

RP represents the $(\nu - 1 - \alpha)$ neutrons provided by the fuel multiplied by σ_f. (The used cross-sections are obviously one-group homogenized over the reactor spectrum.) Higher RP means that transmutation probability increases. (Let us remember that in the past RP was used in order to evaluate the potential of breeding of a core concept. According to the Gen-IV goals [4], the innovative reactors must have a BG = 0 (self-sustaining from the fissile material point of view); so, the neutron excess that in the past was useful in order to breed a fertile blanket is now available for other purposes, mainly transmutation.) Moreover, a positive RP means that the considered material or nuclide produces more neutrons than it consumes and vice versa. As we will see in the next paragraph, RP is a useful parameter to compare the transmutation performance of different kind of core.

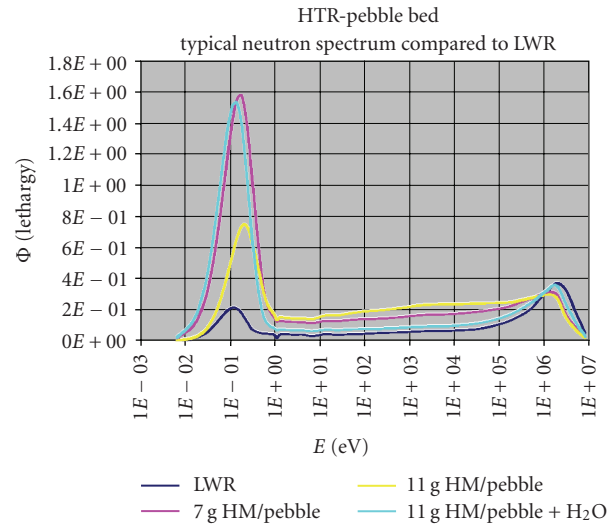

Figure 1: Comparison between LWR and HTR neutron spectrum [10].

Theoretically, it has been proposed [9] also to convert by neutron capture the MA in nuclides with a spontaneous fission probability of 100% (i.e., some isotopes of Bk and Cf), in order to obtain a complete transmutation but it is very challenging from the technological viewpoint.

2.3. Innovative gas-cooled thermal and fast reactors

HTRs are helium-cooled, graphite-moderated high-temperature reactors. These peculiar characteristics have many positive consequences also from the neutronic point of view as follows.

(i) The use of helium as coolant and of graphite as moderator and structural material entails reduced parasitic captures and then a very good neutron economy.

(ii) Moderator separated from a neutronically inert coolant allows to change the lattice parameters without changing dramatically the cooling conditions. This implies a very large flexibility in the choice of the fuel and of the fuel cycle (e.g., HTR can be loaded by Pu without fertile material). (If a loss of coolant occur, the spectral shift is less important than in an LWR and the void coefficient remains negative [1]. Moreover, the spectrum of GCFR is harder than that of an SFR.)

HTRs allow obtaining a very high burnup (up to 750 GWD/tHM when fuelled by PuO_2) thanks to the irradiation endurance of the coated particles. This fact implies higher fluence than in LWR, with a beneficial effect on the transmutation capability. Moreover, HTR has a slightly epithermal spectrum if compared with LWR (Figure 1).

The neutron density in the slowing down range is higher in HTR than in LWR, because the mean lethargic increase of the neutrons is higher with hydrogen than with carbon.

Table 1: Reactivity parameter for some actinides in a different kind of high temperature gas reactor [11].

	Np^{237}	Pu^{238}	Pu^{239}	Pu^{240}	Pu^{241}	Pu^{242}	Am^{243}	Cm^{244}
RP HTR	−27.0	−53.1	+181.1	−143.3	+212.6	-46.0	−82.5	−25.5
RP GCFR	+1.40	−1.40	+3.17	+0.01	+5.40	−0.07	−1.50	+0.21

Nevertheless, the thermal peak in LWR is smaller because of capture by hydrogen nuclei. Thus, HTR seems to have a better transmutation capability than LWR.

The aim of the GCFR concept is coupling the positive characteristics of the helium-cooled reactors (high temperature, chemical and neutronic inertia of the coolant) with those of the fast reactors (better neutron economy and great possibility to choice structural and fuel materials). (Due to He, GCFR has, e.g., a lower (positive) void coefficient than that of a typical sodium-cooled fast reactor.)

It is useful to show the RP for some relevant actinides, calculated over the spectrum of a pebble-bed HTR and a plate-type GCFR, Table 1.

It is clear that almost all the actinide nuclide in the fast spectrum of GCFR produce more neutron than those they consume. Nevertheless, in order to obtain an efficient transmutation to fulfil the previous conditions, the use of GCFR is necessary but not enough, as we will illustrate in the next paragraph.

2.4. The dedicated assembly concept: a way to increase advantages minimizing drawbacks

As already mentioned, thermal reactors are characterized by very large cross-sections but low fluence; while in fast reactor, the fluence is higher but the cross-sections of the nuclides are low, especially these ones of some MA. Because both high fluence and high cross-sections are requested in order to obtain a good transmutation rate, it seems to be useful to adopt some different moderated assemblies in the core of a fast reactor, in order to couple high fluence with high cross-sections. At present, many concepts of dedicated assembly have been designed for LMFBR but also for GCFR (see, e.g., [12]). However, while a moderated dedicated assembly enhances greatly the transmutation efficiency for nuclide like Np^{237} and Am^{241}, it has no effect or a negative one in the case of MA with low cross-section for all energy ranges as Cm^{244} or Cm^{246}. Of course, many researches are still to be performed on this topic.

2.5. Challenges

TRU loading is challenging from the safety point of view. In fact, TRUs are material characterized by a low delayed neutron fraction and are composed by lots of nuclides with different behavior in the resonance region. (In fact, the fission-yield of the precursor nuclei varies with both the type of fissioned-nuclide and the energy of the neutrons inducing fission.) Moreover, concerning thermal reactors, if a Pu+MA fuel is used, a higher enrichment in fissile nuclides is requested than in UO_x fuel, because TRU nuclides have generally a higher capture-to-fission ratio.

Table 2

(a) Delayed neutron fraction (ν_D is the number of delayed neutrons per fission, ν_{total} is the total number of neutrons per fission) [13].

Isotope	ν_D/ν_{total}
U^{238}	0.0151
Th^{232}	0.0209
U^{235}	0.00673
Pu^{239}	0.00187
Pu^{241}	0.00462
Pu^{242}	0.00573
Np^{237}	0.00334
Am^{241}	0.00114
Am^{243}	0.00198
Cm^{242}	0.00033

(b) Example of delayed neutrons fraction [13].

Example		
⇒10% fertile fission raises β in fertile containing fast reactor fuel to:		
$\beta(U^{235})$		$\beta(Pu^{239})$
0.10·0.0151	+	0.90·0.00187
= 0.00151	+	0.00168
= 0.00319		
(Nearly double β vis-à-vis fertile-free fuel		

Fertile material like U^{238} or Th^{232} has a positive effect both on delayed neutron fraction and Doppler feedback, so it can "counterbalance" the effect of the TRU load. The spectrum of HTRs makes the Doppler coefficient strong negative, so that HTRs can be loaded with fertile-free fuel [1]. In GCFR, the high mass of DU in the core has a beneficial effect on the safety parameters; nevertheless further studies are still needed.

The following Table 2 shows the effect of fertile material in the fuel on the total delayed neutron fraction.

3. THE LEVEL OF MINE (LOM) CONCEPT AS REFERENCE PARAMETER: DEFINITION AND DISCUSSION

3.1. Radiotoxicity

Radiotoxicity is a measure for the dose that a human suffers when a certain amount of radioactive nuclides enters the body [1]. The activity of the material, the half-life of its constituent nuclides, the type of radiation, the energy of the emitted particles, the way the radionuclides enter the human body (inhalation/ingestion), the organs that are exposed

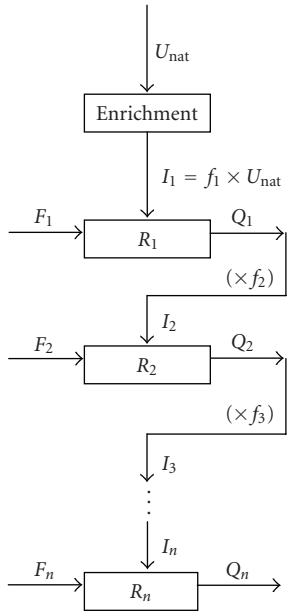

Figure 2: Sketch for LOM calculation.

to the radiation, and the time that the nuclides stay in different organs (biological half-lives) determine the value of this parameter. However, we should not forget that radiotoxicity indicates a potential hazard upon ingestion and/or inhalation, thus if the radionuclides are sufficiently separated from the biosphere, no dose is suffered [1].

3.2. Level-of-mine balancing time

Nevertheless, it is difficult to guarantee the perfect integrity of a human-made confinement beyond 10·000 years [3], then in international context the LOM is used as reference parameter. A reactor or fuel cycle has a positive impact on long-term spent fuel management if it reduces the time that the spent fuel takes to reach the radiotoxicity level of the original uranium ore from which is extracted (see [14], level of mine balancing time (LOMBT)). Because the level of mine is the radiotoxicity of a quantity of natural uranium, it is expressed in Sv. The LOMBT dimension is a time usually expressed in years.

In order to find the LOMBT of the spent fuel from the irradiation cycles showed in the following paragraphs, we have had to calculate the corresponding LOM. We assumed 20 mSv/gU as radiotoxicity of natural uranium [15], while we have neglected the radiotoxicity of thorium, if present. Consider, for instance, a quantity of natural uranium that is enriched and then used as fuel in a chain of reactors (Figure 2).

The radiotoxicity of SNF will depend by the initial fuel composition, the kind of reactor, and the burnup. The corresponding level of mine is obtained calculating the mass of natural uranium that generated the considered quantity of SNF.

This equivalent natural uranium is given by going backward in the following recursive system:

$$\begin{aligned} I_i &= Q_{i-1} \cdot f_i, \\ Q_i &= (I_i + F_i) \cdot b_i, \end{aligned} \tag{6}$$

where

(1) R_i is the i_{th} reactor;

(2) I_i is the fuel loaded in the n_{th} reactor (then let us assume $I_0 = U_{\text{nat}}$);

(3) f_i is the ratio between the input HM mass for the i_{th} reactor and the output HM mass of the $(i-1)_{\text{th}}$ reactor;

(4) F_i is the natural uranium quantity equivalent to be added to the spent fuel from the $(n-1)_{\text{th}}$ in order to manufacture the fuel of the n_{th} reactor;

(5) b_i is the i_{th} reactor burnup expressed as mass of HM discharged/mass of HM loaded (of course $b_0 = 1$);

(6) Q_i is the fuel discharged from the n_{th} reactor.

After having found the $I_0 = U_{\text{nat}}$ mass (expressed in grams), the LOM is obtained as follows:

$$\text{LOM} = U_{\text{nat}} \cdot 20\,\text{mSv/g}U_{\text{nat}}. \tag{7}$$

4. COMPUTER CODES USED

4.1. MCNP-4B

We used MCNP mainly as a part of MONTEBURNS or MCB codes but also to perform some preliminary evaluations on initial k_{eff} values. MCNP [16] is a general-purpose Monte Carlo N-Particle code that can be used for neutron, photon, electron, or coupled neutron/photon/electron transport, including the capability to calculate eigenvalues for critical systems.

The code treats an arbitrary three-dimensional configuration of materials in geometric cells bounded by first- and second-degree surfaces and fourth-degree elliptical tori.

Pointwise cross-section data are used. For neutrons, all reactions given in a particular cross-section file (such as ENDF/B-VI) are accounted for. Thermal neutrons are described by both the free gas and $S(\alpha, \beta)$ models. For photons, the code takes account of incoherent and coherent scattering, the possibility of fluorescent emission after photoelectric absorption, pair production, and bremsstrahlung. A continuous slowing down model is used for electron transport that includes positrons, x-rays, and bremsstrahlung but does not include external or self-induced fields.

Important standard features that make MCNP very versatile and easy to use include a powerful general source, criticality source, and surface source; both geometry and output tally plotters; a rich collection of variance reduction techniques; a flexible tally structure; and an extensive collection of cross-section data.

4.2. ORIGEN2.1

We used ORIGEN mainly as a part of MONTEBURNS code. ORIGEN [17, 18] is a computer code system for calculating the buildup, decay, and processing of radioactive materials. ORIGEN2 is a revised version of the original ORIGEN and incorporates updates of the reactor models, cross-sections, fission product yields, decay data, and decay photon data, as well as the source code. ORIGEN2.1 replaces ORIGEN and includes additional libraries for standard and extended-burnup PWR and BWR calculations, which are documented in ORNL/TM-11018. ORIGEN2.1 was first released in August 1991.

ORIGEN uses a matrix exponential method to solve a large system of coupled, linear, first-order ordinary differential equations with constant coefficients. ORIGEN2 has been variably dimensioned to allow the user to tailor the size of the executable module to the problem size and/or the available computer space. Dimensioned arrays have been set large enough to handle almost any size problem, using virtual memory capabilities. The user is provided with much of the framework necessary to put some of the arrays to several different uses, call for the subroutines that perform the desired operations, and provide a mechanism to execute multiple ORIGEN2 problems with a single job.

ORIGEN2 solves Bateman's equations by matrix exponential method. The system of differential equations can be written as follows:

$$\dot{X}(t) = AX(t), \tag{8}$$

where

(1) X is the column vector of the nuclide concentration;

(2) A is the transition matrix containing the transformation rates.

This equation has the solution

$$X(t) = X(0)\cdot e^{At}, \tag{9}$$

where $X(0)$ is the vector of initial nuclide concentrations.

The matrix exponential method generates $X(t)$ expanding in series the exponential function (incorporating enough terms in order to obtain the desired accuracy):

$$X(t) = X(0)\left[I + At + \frac{1}{2}(At)^2 + \cdots\right]. \tag{10}$$

4.3. MONTEBURNS1.0

We used MONTEBURNS in order to perform all the burnup calculations except for those ones referred to [19, 20].

MONTEBURNS [21] couples MCNP [16] and ORIGEN [17] codes through MONTEB utility and a PERL [22] procedure. MONTEBURNS produces a large number of criticality and burnup results based on various material feed/removal specifications, power(s), and time intervals.

MONTEBURNS [18] processes input from the user that specifies the system geometry, initial material compositions, feed/removal specifications, and other code-specific parameters. Various results from MCNP, ORIGEN2, and other calculations are then output successively as the code runs. The principle function of MONTEBURNS is to transfer one-group cross-section and flux values from MCNP to ORIGEN2, and then transfer the resulting material compositions (after irradiation and/or decay) from ORIGEN2 back to MCNP in a repeated, cyclic fashion (a simple predictor-corrector method is used during this process).

The depletion equations use fluxes, nuclide number densities and cross-sections to determine the time-dependent nuclide inventory. The simplified one-group depletion equation is [23]

$$\frac{dN(r,t)}{dt} = -\varphi(r,t)\cdot\sigma(r)\cdot N(r,t). \tag{11}$$

The solution for nuclide density is

$$N(r,t) = N_0(r)e^{-\sigma(r)\int_{t_1}^{t_2}\varphi(r,t)dt}. \tag{12}$$

Thus, the change in nuclide concentration is dependent on the fluence. However, the time-dependent flux depends on the nuclide density, then the previous equation is not linear. In order to make the equation linear, it is necessary to assume the flux constant throughout the burn step equal to the average flux over the entire burn step:

$$N(r,t) = N_0(r)e^{-\sigma(r)\varphi(r)_{\text{average}}}. \tag{13}$$

MONTEBURNS, as already anticipated, makes an approximation of the average flux behavior by using a predictor-corrector method as follows.

(1) Firstly, MCNP runs in order to calculate the initial macroscopic one-group cross-sections and flux over the core.

(2) Then, ORIGEN is executed in order to perform a burnup calculation over the half time step $[t(i)\rightarrow t(i+1/2)]$: this is the "Predictor-step."

(3) Fluxes and collision densities are recalculated by MCNP at the half-time step (based on the nuclide inventory found by ORIGEN during the predictor step).

(4) These fluxes and collision densities are used by ORIGEN to perform the burnup calculation over the full time step $[t(i)\rightarrow t(i+1)]$: this is the "Corrector-step."

Obviously, the time steps cannot be too long, in order to avoid unacceptable changes of the flux shape.

4.4. MCB

We used MCB in order to perform the burnup calculations referred to [19, 20].

MCB [24] is a general-purpose MC code used to calculate the evolution in time of nuclide density and composition, taking burnup, and decay into account. It was developed

by Cetnar, Gudowski, and Wallenius and can perform both eigenvalue calculations for critical and subcritical systems as well and neutron transport calculations in fixed source mode or k-code mode, to obtain reaction rates and energy deposition that are necessary for burnup calculations. This code integrates the well-known code MCNP [16], version 4C, which is used for neutron transport calculation, and a novel TTA code [25], which serves for density evolution calculation, including formation and analysis of the transmutation chain. MCB is compatible with MCNP and preserves its structure, so that a complete burnup calculation can be performed in one single run, requiring just slight modification of an MCNP input file. The code was extensively tested by the authors in benchmark calculations and reactor core designing. The general conclusion from practical application shows that MCB version 1C produces valuable results that are physically consistent, and the correctness of physical model applied has been proved. This version of MCB can also simulate material processing including continuous feeding of materials that is the most important for our purpose. Development of the code was addressed towards improving calculation effectiveness, system diagnostic, and physical model for rigorous treatment but also providing simplified model option for quick design studies or benchmarks. The TTA code [25] implements a new technique of Bateman equation solutions which adequately represents the physics of the transmutation process, and thus it is capable of delivering additional information of the transmutation process when compared to the matrix method. This approach allows the user to obtain qualitative and quantitative trajectories of transmutations additionally to densities of transmuted nuclides.

4.5. WIMSD5B.12

We have used WIMS code in order to perform some preliminary parametric evaluations on HTR and GCFR cores. Winfrith improved multigroup scheme (WIMSD) [26] is a deterministic code that sets out to calculate neutron flux distribution and values of k-infinity or k-effective. To do this it has to solve a mathematical form of the neutron transport equation. WIMSD is a very useful tool to perform quickly calculation for analysis of experiments, criticality and power reactor design, assessment and operation. There are currently three versions of WIMS, namely WIMSD, WIMS-E (now up to version WIMS-8), and LWRWIMS. All versions use a WIMS library, initially in 69 energy groups and containing equivalent data. WIMSD (originally WIMS, followed by versions A to D) was developed from $1963 \div 5$, with some later improvements. It is a single code with a limited number of options, is fast in execution, and is recommended for straightforward "pin-cell" and cluster calculations. In the late 1960s, development on WIMS-E began to provide a modular code scheme giving the user much more flexibility in choosing his options. Execution time may be much longer than those for WIMSD so that WIMS-E is used for problems that WIMSD cannot calculate adequately. LWRWIMS has a structure which is based on that of WIMS-E although the modules are bound together in a single program. Development started in the early 1970s and has continued at a low level since then. LWRWIMS was written specifically for light water reactor geometries. In summary, WIMSD is useful for homogeneous slab, pin-cell or cylindrical cluster geometries. It has been developed substantially for GCR, AGR, CANDU, and RBMK, although it can be used with caution also for other kinds of reactor.

4.6. XSDRNPM

We have used XSDRNPM code in order to perform some preliminary parametric evaluations on GCFR cores. XSDRNPM [27] is a discrete-ordinates code that solves the one-dimensional Boltzmann equation in slab, cylindrical, or spherical coordinates. Alternatively, the user can select *p1* diffusion theory, infinite medium theory, or *Bn* theory. A variety of calculational types is available, including fixed source, eigenvalue, or "search" calculations. In SCALE, XSDRNPM is used for several purposes: eigenvalue (k_{eff}) determination, cross-section collapsing, shielding analysis, and for producing bias factors for use in Monte Carlo shielding calculations.

4.7. CARL

We have developed CARL code in order to perform in a quick but reliable way all the radiotoxicity evaluations for the spent fuel (outside the reactors). Calculation of radiotoxicities lifetime (CARL) code was originally (in 2003) developed for master degree thesis purposes [19] in *MATHCAD* environment. It originally calculated the radiotoxic (ingestion) inventory evolution versus time of a given radionuclide composition. It was developed in order to perform the complex calculations regarding the nuclear spent fuel hazard versus time (it was supposed, prudentially, that water could, in a remote future, corrode casks, and transport radionuclides to biosphere). It is well known in fact that the danger coming from nuclear waste over time decreases continuously due to radioactive decay. Version 2 of the code was developed in *MATLAB* environment (MATLAB 6.5, release 13 or higher required), and was strongly enhanced: it performs in addition to radiotoxicity, also activity, dose and decay power calculations; it displays also the "*Gamma Spectrum*," a 3D plot indicating the activity of gamma rays versus time and radiation energy. Code's input can be given manually (in grams for every nuclide), or by file (by using MCB-1C, MONTEBURNS-1.0 output file, or CARL input file).

The present version of the code (2.2) presents the following additional features: it includes U^{232} isotope (very useful in thorium fuel cycles calculations) and common nuclear reactors activation materials (Cr^{51}, Mn^{56}, Fe^{59}, Co^{60}, Ni^{65}, Cu^{64}, Zn^{65}, Zn^{69}, Zr^{95}, Mo^{99}, Ta^{182}, W^{187}) [28], and displays also two additional plots indicating the *equivalent gamma dose rate* (in mSv/h) versus time (the distance considered, in meters, is assigned in input), both in air and in concrete/rock; moreover it displays the masses (in grams) in the text output file of all the radionuclides at the various logarithmically spaced time points.

The calculation procedure implemented by CARL 2.2 solves the *Bateman equations* for radioactive decay chains. If we have chain radioactive decays, and we refer to the initial nucleus as 1, to the succeeding generations (daughter) as 2, granddaughter as 3, and so forth, that is,

$$1 \longrightarrow 2 \longrightarrow 3 \longrightarrow 4 \longrightarrow \cdots, \tag{14}$$

it will be [28]

$$dN_i = \lambda_{i-1} N_{i-1} dt - \lambda_i N_i dt, \tag{15}$$

(every nuclide will decay and will be produced from its parent decay).

If N_0 is the number of initial nuclei of type 1 and none of the other types are present, the activity of the nth nuclide will be

$$A_n = N_0 \sum_{i=1}^{n} c_i e^{-\lambda_i t} = N_0 \left(c_1 e^{-\lambda_1 t} + c_2 e^{-\lambda_2 t} + \cdots + c_n e^{-\lambda_n t}\right),$$
$$c_m = \frac{\prod_{i=1}^{n} \lambda_i}{\prod_{i=1, i\neq m}^{n} (\lambda_i - \lambda_m)} = \frac{\lambda_1 \lambda_2 \lambda_3 \cdots \lambda_n}{(\lambda_1 - \lambda_m)(\lambda_2 - \lambda_m)\cdots(\lambda_n - \lambda_m)}. \tag{16}$$

The code divides the time interval in 50 logarithmically spaced points (by default, which obviously may be changed by the user). Activities are then multiplied for the *dose factors* (Sv/Bq) [28] to obtain the (ingestion) radiotoxicities. Partial activities and radiotoxicities are summed up to obtain totals.

Then code multiplies the calculated activities for the respective decay energies (expressed in MeV [28]) and for $1.6 \cdot 10^{-13}$ to obtain watts from MeV/sec (1 eV = $1.6 \cdot 10^{-19}$ J).

To obtain the integrated dose to materials from time 0 to t, we have to integrate the activity, multiply the result for the energy of disintegration (in MeV) and divide for the number of grams to obtain MeV/g; we will multiply the result by $1.6 \cdot 10^{-10}$ to express the integrated dose versus time in *Grays* (1 Gray = 1 J/Kg = 100 rad):

$$D = \frac{\left(\int_0^t A dt\right) \cdot E \cdot 1.6 \cdot 10^{-10}}{g} = \frac{\left(\int_0^t \lambda N_0 e^{-\lambda t} dt\right) \cdot E \cdot 1.6 \cdot 10^{-10}}{g}$$
$$= \frac{N_0 \left(1 - e^{-\lambda t}\right) \cdot E \cdot 1.6 \cdot 10^{-10}}{g} (\text{Grays}). \tag{17}$$

Volumes of water are calculated assuming a daily assumption of 2.5 litres of water by ingestion, that is, 913 litres/year; dividing this value for the input *annual limit* (in Sv/year), we obtain the number of litres/Sv to maintain the water potable. Divided by total nuclides mass and multiplying by 10^6 to obtain m^3/ton, we have

$$\text{Volume\_Water} = \frac{\text{Total\_Radiotoxicity} \cdot (913/\text{limit})}{\text{Total\_Mass}} \cdot 10^6 (\text{m}^3/\text{ton}). \tag{18}$$

The *Gamma Spectrum* represents only the gamma energy of the radiations (which may be dangerous due to their penetration power), interesting in case of isotopes handling (e.g., nuclear spent fuel). Only principal energy decays are considered.

Equivalent Dose Rate could be calculated as follows: if we consider a gamma-ray intensity of I_γ photons/$m^2 \cdot$ s with an energy of E_γ MeV, the energy flux will be $I_\gamma E_\gamma$ MeV/m^2 s. The rate of energy deposition per unit volume (in a small volume) will be $I_\gamma E_\gamma \mu_a$ MeV/m^3s, with μ_a as the *linear absorption coefficient* (m^{-1}). If ρ is the density of the material, then $I_\gamma E_\gamma \mu_a / \rho$ will be the rate of energy deposition (MeV/Kg s), and remembering that 1 MeV = 1.60×10^{-13} J and 1rad = 10^{-2} J/Kg, it will be

$$D_\gamma = 1.60 \cdot 10^{-11} \frac{I_\gamma E_\gamma \mu_a}{\rho} [\text{rad/s}] = 5.76 \cdot 10^{-5} \frac{I_\gamma E_\gamma \mu_a}{\rho} [\text{mrad/h}]. \tag{19}$$

Considering that at a distance R from the source the photons are distributed uniformly over a sphere of area $4\pi R^2$, and that travelling trough a medium (e.g.: air or concrete) will be attenuated by the factor $e^{-\mu R}$, it is

$$I_\gamma = \frac{A}{4\pi R^2} e^{-\mu R}. \tag{20}$$

Substituting (20) in (19), it will be

$$\text{A}_{\text{dsorbed}}\text{D}_{\text{ose}}\text{R}_{\text{ate}} = \frac{5.76 \cdot 10^{-5}}{4\pi} \cdot \frac{A E_\gamma \mu_a}{R^2 \rho} e^{-\mu R}$$
$$= 4.58 \cdot 10^{-6} \cdot \frac{A E_\gamma \mu_a}{R^2 \rho} e^{-\mu R} [\text{mrad/h}] \tag{21}$$
$$= 4.58 \cdot 10^{-8} \cdot \frac{A E_\gamma \mu_a}{R^2 \rho} e^{-\mu R} [\text{mSv/h}].$$

The air density considered is 1.225 Kg/m^3 (at room temperature), concrete/rock density 2500 Kg/m^3. The value of μ_{a_air} is 5×10^{-3} m^{-1} for air (an average value in the range 0.1–2.0 MeV, [2]); for concrete, it was considered an HVT (Half Value Thickness) of 5 cm, so $\mu_{a\_\text{concrete}} = \ln(2)/(5 \cdot 10^{-2}) = 13.863$ m^{-1}. Total dose rate is calculated as the sum of every single radionuclide chain contribution. Obviously it is an approximate value.

Radionuclides masses (in grams) in the text output file are calculated from the following equations [28]:

$$A(t) = \lambda N(t),$$
$$N(t) = \frac{A(t)}{\lambda} = \frac{m(t)}{\text{AM}} \cdot \text{NA}, \tag{22}$$
$$m(t) = \frac{A(t) \cdot \text{AM}}{\lambda \cdot \text{NA}},$$

where AM is the atomic mass of the radionuclide, NA the Avogadro's number, and $N(t)$, and $m(t)$, respectively, the number of decaying nuclei and the radionuclide mass at time t.

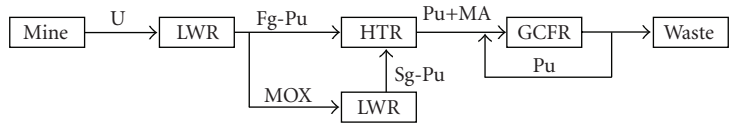

Figure 3: Symbiotic fuel cycles (without or with using MOX in LWR).

Table 3: Summary of the obtained results.

Case	Reactor	Fuel	LOMBT [y]	$\frac{\text{Energy}}{g_{Pu}}$	$\frac{Pu_{out}}{Pu_{in}}$	$\frac{TRU_{out}}{TRU_{in}}$	$\frac{Act_{out}}{Act_{in}}$
1	2	3	4	5	6	7	8
a	HTR	1st g-Pu/Th (1/1)	37982*	60.16 GJ	24.14%	31.75%	63.88%
b	HTR	1st g-Pu/Th (1/2)	37547*	59.40 GJ	27.75%	33.88%	76.25%
c	HTR	1st g-Pu/Th (1/3)	37117*	58.89 GJ	29.06%	34.37%	81.94%
d	GCFR	1st g-Pu**/MA/U^{238} (10/1/40)	9204***	154.44 GJ	85.66%	86.77%	57.78%
e	GCFR	2nd g-Pu†/MA/U^{238} (10/1/40)	9310***	155.26 GJ	85.85%	87.77%	57.57%
f	GCFR‡	2nd g-Pu†/MA/U^{238} (10/1/40)	11860***	105.57 GJ	98.02%	98.95%	70.64%

* In the case of HTR, we assumed a once-through fuel cycle. Consequently, the waste contains Pu, MA, and FP.
** 1st-generation Pu is added to Pu which is already present in the spent fuel of HTR loaded with 1st-generation Pu.
*** In the case of GCFR, we assumed that all the Pu is recycled. Consequently, the waste contains only MA and FP.
† 2nd-generation Pu is added to Pu which is already present in the spent fuel of HTR loaded with 2nd-generation Pu.
‡ In this case, we assumed that thickness of the external layer of the CP is 0.003 mm instead of 0.005 mm (like cases d and e). Therefore the spectrum is not so hard as in case e.

5. ACTIVITY PERFORMED AT THE UNIVERSITY OF PISA

5.1. The HTR as plutonium burner

In order to demonstrate the capability of HTRs to contribute in reducing nuclear waste (actinides in particular), it was decided to analyze Pu-based fuel [14]. In order to validate the used code (namely MONTEBURNS), an international code-to-code benchmark was performed. The obtained results have shown a good agreement between the codes adopted by the different participants, as reported in [29].

Particularly, 1st generation Pu [20] (i.e., Pu deriving from reprocessing typical LWR spent fuel) and 2nd generation Pu [20] (i.e., Pu deriving from the reprocessing of typical MOX spent fuel) were considered.

Therefore the following calculations were performed:

(i) HTR loaded with 1 g/pebble 1st generation Pu, 600 GWd/ton (600 EFPD);

(ii) HTR loaded with 1.5 g/pebble 2nd generation Pu, 430 GWd/ton (645 EFPD).

To check the advantages in using different fuel cycles, the radiotoxicity evolution of spent fuel versus time was evaluated. As reference for radiotoxicity, we, as described above, originally defined [14] the *LOMBT (level of mine balancing time)*, that is, the interval of time necessary for the radiotoxicity of the exhausted fuel to return to the values of the mineral extracted from the mine (in this case of uranium) from which the fuel was generated.

The results show that 1st-generation Pu behaves (in terms of LOMBT) better than 2nd-generation Pu.

In another article [30], we considered the possibility of adopting Th-Pu fuel cycle and, for the first time, the use of a (relatively) simplified LWR-HTR-GCFR symbiotic fuel cycle (Figure 3).

It should be noted that, in the case of HTR, we considered a once-through fuel cycle. Consequently, we assumed that the waste contains Pu, MA, and FP. Instead in the case of GCFR, we considered that all the Pu will be recycled at the end of (each) GCFR step. Consequently, we assumed that the final waste contains only MA and FP.

In Table 3, the obtained results are summarized. In column 7, the ratio between inlet and outlet transuranic elements (Pu+MA) and in column 8 the ratio between inlet and outlet actinides (Th+U+Pu+MA) is shown.

In the case of LWRs spent fuel, the LOMBT is about 250000 years [15]. From Table 3, we can see that this figure of merit (the most important in terms of safety) is significantly reduced (an order of magnitude) using HTR and further (recycling Pu as fuel) by using GCFR to close the cycle.

5.2. The GCFR as actinide burner

In the first calculations (see previous paragraph) on GCFRs concepts, we adopted a simplified model for the GCFR core. In the further calculations, we refined this model, as showed in the following paragraphs.

5.2.1. Comparison among core concepts

Three main core concepts exist for GCFR:

(1) particle-bed core;

(2) pebble-bed core;

(3) plate-type core.

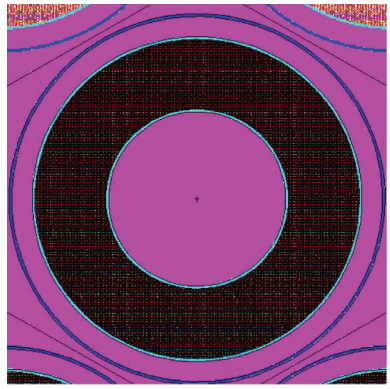

Figure 4: Particle-bed core. The FA is constituted by two walls of porous SiC (in light blue); the CPs (in dark color); an outer wall of SiC (in blue). The purple region is He.

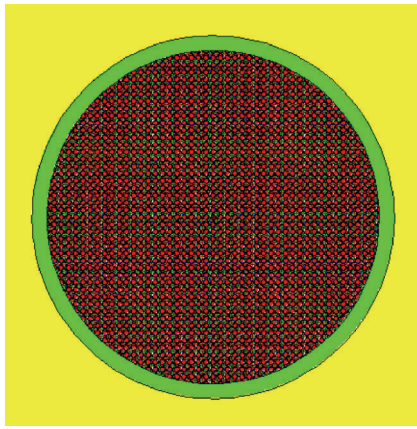

Figure 5: Pebble-bed core: details of a pebble (in the inner part of the sphere there are the CPs, the green shell is the fuel-free zone in C, the yellow region is the coolant He).

The particle-bed core consists of a lattice of annular cylinders filled by CPs. The coated particles are characterized by a larger oxide fuel kernel and few coating layers than those designed for HTGRs [30].

The pebble-bed core is like that proposed in [31], with pebbles filled by a matrix of graphite and CPs with carbide kernels.

The new plate-type concept, proposed recently by CEA [32], is a lattice of hexagonal assemblies. Every assembly contains 21 fuel plates coated by SiC and cooled by He. The fuel is a matrix of (U,Pu)C and SiC [32].

At the begin, we have investigated on these three core concepts to evaluate the actinide-burning capability of these different kinds of GCFR, particularly in order to check that the plate type has really the best waste-transmutation characteristics if compared with the others (as already stated on the basis of some preliminary calculations performed in the frame of GCFR project). In fact, all our successive work is focused on this kind of core, in the frame of the EU GCFR project. Figures 4, 5, and 6 show the core we modelled by MCNP4B code.

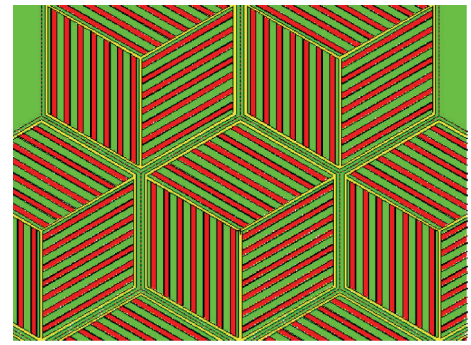

Figure 6: Plate-type core: details of core xy-cross-section (fuel matrix is in red colour, SiC in yellow, and He in green).

In all three cases, the HM part of the fuel is composed by DU and Pu+MA with the isotopic vector of LWR spent fuel. The relative percentages of DU and (Pu+MA) are adjusted in order to obtain criticality.

The main results we found are summarized in Table 4.

Please note that we used as figure of merit the following ratio:

$$\Delta m_i 100/\text{Energy [kg/GWD]}, \tag{23}$$

where

(a) Δm_i is the difference between the loaded mass and the discharged mass in the core for the ith group of nuclides [Kg];

(b) "Energy" indicates the energy produced by the core during irradiation [GWD].

The higher this figure of merit, the better the performance of the core in burning the ith group of nuclide.

As we can see from Table 4, the plate-type core has three main advantages:

(1) a longer fuel cycle thanks to the better conversion fertile-to-fissile of DU;

(2) a smaller initial enrichment in Pu+MA than the pebble-bed type (Pu and MA have a quite different dynamic behaviour than traditional fuel);

(3) a higher consumption of DU. The Pu net consumption is not too high because of the conversion and the subsequent high-fission probability of Pu^{239} and also of the conversion of Np^{237};

(4) a higher consumption of the higher isotopes of Pu and of the MA due to the harder neutron spectrum (Table 5 and Figure 7).

The harder neutron spectrum of the plate-type core is due to the higher volumetric fraction of the fuel than that of structural material (in fact, the structural material is composed by Si and C, which are relatively light nuclei), Table 6.

Please note that the CP-bed core reaches the criticality also with a very low fraction of fuel, thanks to its large size

Table 4: Summary of the comparison of the GCFR core concepts.

	Plate-type GCFR	CP-bed GCFR	PB-GCFR
Power [MW_{th}]	600	2400	300
Power Density [W/cc]	100	50	50
Irradiation time length [days]	2944	1938	1138
Pu+MA charge (atomic fraction)	20%	20%	25%
DU initial mass[kg]	12531.5	17543.8	5894.049
DU final mass [kg]	11012.1	17034.6	5610.23
Pu initial mass [kg]	2842.4	3966	1776.04
Pu final mass [kg]	2699	3898	1708.45
MA initial mass [kg]	299.1	417.7	186.615
MA final mass [kg]	248.49	458.11	180.979
Δm_{DU}/Energy [kg·100/GWD]	86.02	10.95	83.17
Δm_{Pu}/Energy [kg·100/GWD]	8.12	1.46	19.81
Δm_{MA}/Energy [kg·100/GWD]	2.87	−0.87	1.64

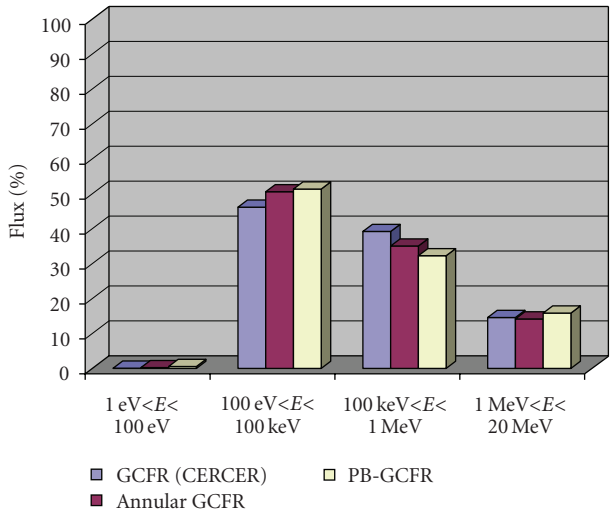

Figure 7: Comparison of the mean neutron spectra: the plate-type core has the harder spectrum (groups over 100 keV).

Table 5: (Δm·100/GWD) of the different core concepts for the main nuclides.

Nuclide	Plate-type	CP-bed	Pebble-bed
U^{238}	**84.92**	**10.75**	**81.88**
Np^{237}	**4.40**	**0.80**	**7.30**
Pu^{238}	−2.58	−0.71	−5.62
Pu^{239}	**3.40**	0	**20.04**
Pu^{240}	−3.96	−1.10	−11.06
Pu^{241}	**11.10**	**3.40**	**17.84**
Pu^{242}	**0.17**	−0.13	−1.38
Am^{241}	**0.31**	−1.33	−2.00
Am^{243}	**0.36**	**0.04**	**0.17**
Cm^{244}	−1.29	−0.18	−2.04

(2400 MW_{th} with a power density of 50 W/cm^3), that minimizes the neutron losses.

Table 6: Volumetric percentages of the materials in the core concepts analyzed.

	Plate-type	CP-bed	Pebble-bed
Fuel (HM oxide or carbide) % vol.	24.5	9.5	15
Coolant % vol.	55	74	39
Structural mat. % vol.	20.5	16.5	46

These positive characteristics justify a deeper analysis of this kind of core that will be performed in the following paragraphs.

5.2.2. *Benchmarks and codes validation*

GCFR is a new concept of core that has not already been studied with the standard computer codes for neutronic analyses. Then, in the frame of the EU GCFR project, we have participated to a code-to-code benchmark using the reference core configuration (plate-type GCFR), proposed by CEA [32]. This comparison supplied very interesting results, because the core has been modelled both with an MC code (MCNP) and with a 1D deterministic code (XSDRNPM). The differences in k_{eff} and in the isotopic evolution of the fuel during burnup are very small, mainly due to the different set of cross-sections used. In fact, the agreement has been very good for U, Pu^{239}, and Pu^{240}, while the biggest difference has been found regarding the MA and the higher isotopes of Pu. That is not surprising, because the cross-sections of these nuclides are those with the higher uncertainties and the higher differences among the different sets [33].

The good agreement between the 3D heterogeneous model and the 1D homogeneous model is probably due to the presence of a fast spectrum: the mean free path of the neutrons is comparable with the typical dimensions of the core, so that the collision densities in both configurations are similar. This is a very promising result, because the deterministic codes (XSDRNPM, WIMS, etc.) allow to perform

Table 7: Out/in ratio (%) for the main nuclides in multiple recycling.

	1st cycle	2nd cycle	3rd cycle	Total
Length [days]	2944	1863	1738	6545
(Pu+MA)C atomic fract. (%)	20	18.4	18.3	—
$U^{238}{}_{out}/U^{238}{}_{in}$ (%)	88	91	92	73.7
$Np^{237}{}_{out}/Np^{237}{}_{in}$ (%)	46	61	66	18.5
$Pu^{238}{}_{out}/Pu^{238}{}_{in}$ (%)	163	97	89	140.7
$Pu^{239}{}_{out}/Pu^{239}{}_{in}$ (%)	96	101	101	97.9
$Pu^{240}{}_{out}/Pu^{240}{}_{in}$ (%)	110	105	104	120
$Pu^{241}{}_{out}/Pu^{241}{}_{in}$ (%)	45	85	98	37.5
$Pu^{242}{}_{out}/Pu^{242}{}_{in}$ (%)	98	93	93	84.8
$Am^{241}{}_{out}/Am^{241}{}_{in}$ (%)	94	80	85	63.9
$Am^{243}{}_{out}/Am^{243}{}_{in}$ (%)	87	94	94	76.9
$Cm^{244}{}_{out}/Cm^{244}{}_{in}$ (%)	245	118	106	306.4

preliminary evaluations in a quicker way: we can so use those tools with confidence.

5.2.3. Multiple recycling on GCFR: a preliminary evaluation

As already explained, an important aim of the GCFR core design is to obtain a self-sustaining core fed with fertile material. The batches discharged from GCFR would be reprocessed, recovering all the HMs, and eliminating the FPs as waste. Then the HMs would be reused in order to fabricate new fuel, adding DU to replace the material consumed by fission. We have performed some calculations in order to evaluate the fuel behavior during multiple recycling, starting with an initial composition with 80% DU and 20% (Pu+MA) from LWR. Moreover, we have neglected the cooling time between an irradiation cycle and the fact that matter will be deepened in the frame of the optimization of the entire fuel cycle, as future work. Here it is sufficient to remember that few years of decay causes mainly the buildup of Am^{241} from Pu^{241} (half-life 14.4 years) and Pu^{238} from Cm^{242} (half-life 163 days). We have performed three complete irradiation cycles, the main results are summarized in Table 7.

This core shows a very good conversion capability that can be described as follows (Table 7):

(a) the added DU initial fraction increases from a cycle to the other because the reduced destruction of Pu fissile isotopes (i.e., Pu^{239} and Pu^{241}) and the increased burnup of those fertile (i.e., Pu^{240} and Pu^{242}) allow to obtain criticality in the successive cycles also with lower percentages of (Pu+MA);

(b) the lower initial content of Pu+MA causes a decrease of the single cycle step length;

(c) except the fissile Pu nuclides, all the isotopes show a progressive decrease either of their quantity or, at least, of their growing rate (i.e., Pu^{240} and Cm^{244}) from a cycle to the other.

This will not be a real problem. In fact we are not sure that it will be possible to reach a so long irradiation cycle length (due to radiation damage of the core materials). These trends are encouraging: optimizing the parameters of the fuel and the cycle; and using some dedicated assemblies, there are good possibilities of further actinide reduction by GCFR.

5.3. Symbiotic fuel cycles

Although [34] water-cooled thermal reactors have reached a high stage of development and can (economically) give a significant contribution to the world energy supply, the efficient utilization of U or Th resources and the long-term management of the waste are still a challenge. As stated before, in the short term, even if U availability seems to be adequate to fuel the continuing installation of thermal reactors, this cannot be sustained for the next centuries. Future improvements in the performance of thermal reactors can be reached particularly in terms of increased efficiency through higher temperatures of the HTR system. Furthermore, by using the fast reactors features and multiple symbiotic cycles, the utilization of uranium resources could be highly enhanced in addition to a further waste reduction.

A symbiotic fuel cycle is a strategically planned chain, where the output of a reactor is the input of the following. Each link of such a chain is a different kind of reactor (e.g., LWR, HTR, or FR, etc.), because each one is able to do a different task. Of course, between two different steps, the fuel has to be cooled and reprocessed. Further data on chemical aspects of these reprocess steps are available in the international literature (e.g., documents from EU projects on HTR).

In this way, the waste radiotoxicity growth can be reduced by recycling both Pu and MA, producing, at the same time, energy.

5.3.1. A symbiotic LWR-HTR-GCFR fuel cycle

As shown, in the past, our group has already performed similar calculations using LWR-HTR-GCFR fuel cycles [30]. In Figure 8, a flowchart of our proposed symbiotic cycle is shown.

We have modeled the core of a pebble-bed HTR (like a 233 MW_{th} PBMR) [34], whose CPs are loaded by Pu+MA coming from LWR (the considered burnup is the typical value of 33 GWD/tU). The chemical form of the fuel kernel is (Pu, MA)O_2. Thus, we performed for this HTR core the burnup calculation until k_{eff} became less than 1 (about 500 GWD/tHM). The isotopic composition we obtained constitutes the fissile material to be added to depleted uranium in the GCFR fuel. Finally, we have performed the burnup calculation of the GCFR core until k_{eff} became less than 1 (about 188 GWD/tHM) and evaluated the radiotoxicity of the final waste (i.e., only the FPs in the frame of the *full actinides recycle* strategy). For criticality reasons, we chose for GCFR a fuel composition constituted by 30% as atomic fraction of Pu+MA (TRU) and 70% of DU (DU contains 0.25% in U^{235}). Please note that DU represents a

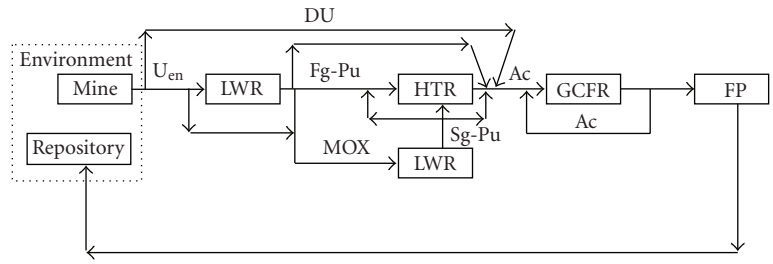

Figure 8: Symbiotic fuel cycle LWR-HTR-GCFR [34].

Table 8: TRU isotopic vectors.

Mass fraction	Spent LWR	Spent HTR
Np^{237}	0.046	0.056
Pu^{238}	0.023	0.073
Pu^{239}	0.490	0.074
Pu^{240}	0.215	0.313
Pu^{241}	0.114	0.18
Pu^{242}	0.062	0.20
Am^{241}	0.028	0.0001
Am^{243}	0.016	0.04
Cm^{242}	—	0.013
Cm^{244}	0.005	0.043
Cm^{245}	—	0.0079

material not more useful in order to produce energy in a "classical" way. Therefore, it has a very low cost. The isotopic vectors of TRU resulting, respectively, from LWR and HTR that we used are shown in Table 8.

Please note that the burnup calculation on GCFR here shown is only the first of a series performed in the frame of the Generation IV Initiative. This strategy represents the so called *full actinide recycle* strategy, proposed by CEA for this kind of reactor. A preliminary study of this strategy in GCFR is shown in the previous paragraphs and summarized in Table 7.

As already described, this concept consists in adding all the actinides coming from GCFR spent fuel to DU that substitutes the mass of fuel lost as fission products. If the efficiency of the separation process were 1, the waste would be (ideally) composed by FP only, while the actinides would always be reused in the reactor as new fuel.

5.3.2. LOMBT evaluations for LWR-HTR-GCFR fuel cycles

To check the advantages of the chosen fuel cycles, we mainly took into account the radiotoxicity evolution of the spent fuel versus time. As already anticipated, please remember that as reference for radiotoxicity, we defined [14] the level-of-mine balancing time (LOMBT). This value is linked to the LOM definition, value characteristic of the type of fuel cycle and it is not easily defined (due to its oscillation range). However, in this paper, we adopt the LOM only as a conceptual reference level.

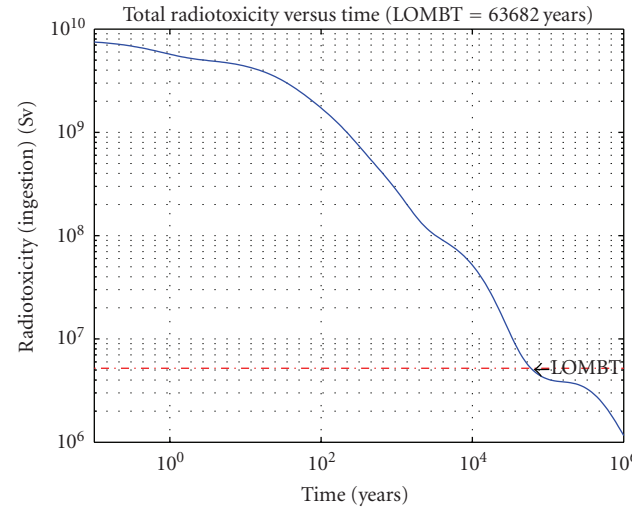

Figure 9: Spent fuel radiotoxicity versus time for HTR, intermediate step ("*waste*" = Pu+MA+FP): LOMBT = 63682 years.

At the end of the single steps we consider as waste the following:

(1) Pu+MA+FP in the case of HTR, because HTR has a "single-step" fuel cycle (i.e., a given quantity of material spends only a burnup cycle in this kind of reactor);

(2) FP in the case of GCFR; in fact, in GCFR, the *full actinide recycle* is foreseen (i.e., all the actinides from an irradiation step will be mixed to new DU in the "fresh" fuel for cycle continuation).

However, in this paper, we have limited the analyses to the first irradiation cycle in GCFR without considering what happens with the multiple recycles of the fuel. The evaluations of the successive irradiation cycles are in progress.

Table 9 gathers the results we found; while in Figures 9 and 10, two typical CARL output graphs are showed.

This strategy couples the advantages of both the HTR neutron spectrum (good performance in Pu, Np^{237} and Am^{241} burning) and the GCFR spectrum (capability of burning the higher Pu isotopes and of decreasing the Cm^{244} growing rate).

Table 9: Summary of the obtained results.

	HTR (513 EFPD)	GCFR (4950 EFPD)	Symbiotic cycle*
LOMBT [years]	63˙682 (waste = FP+HM)	159 (waste = FP**)	159 (waste = FP**)
$Np^{237}{}_{out}/Np^{237}{}_{in}$	66%	27%	18%
$Pu^{238}{}_{out}/Pu^{238}{}_{in}$	165%	75%	123%
$Pu^{239}{}_{out}/Pu^{239}{}_{in}$	81%	306%	248%
$Pu^{240}{}_{out}/Pu^{240}{}_{in}$	77%	73%	56%
$Pu^{241}{}_{out}/Pu^{241}{}_{in}$	80%	26%	20%
$Pu^{242}{}_{out}/Pu^{242}{}_{in}$	170%	72%	122%
$Am^{241}{}_{out}/Am^{241}{}_{in}$	21%	243%	51%
$Am^{243}{}_{out}/Am^{243}{}_{in}$	126%	83%	104%
$Cm^{244}{}_{out}/Cm^{244}{}_{in}$	412%	102%	420%

* In this case, there is no indication about EFPD because the real cycle is made of burnup days inside the reactors plus days out-of-pile (mainly due to recycling times).

** The fission products considered here are the following: Rb^{87}, Sr^{90}, Zr^{93}, Nb^{94}, Tc^{99}, Pd^{107}, Sn^{126}, I^{129}, Cs^{135}, Cs^{137}, Sm^{147}, Sm^{151}, and Eu^{154}.

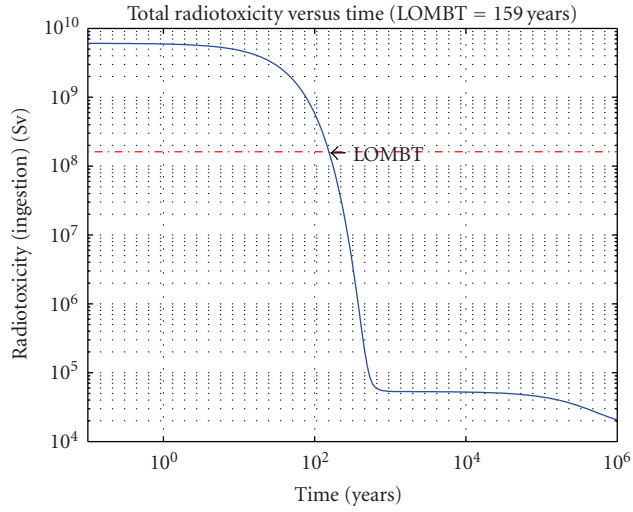

Figure 10: Spent fuel radiotoxicity versus time for GCFR, "final" step ("*waste*" = FP): LOMBT = 159 years. (The fission products considered here are the following: Rb^{87}, Sr^{90}, Zr^{93}, Nb^{94}, Tc^{99}, Pd^{107}, Sn^{126}, I^{129}, Cs^{135}, Cs^{137}, Sm^{147}, Sm^{151}, and Eu^{154}.) (If we would consider as waste FP and MA, the LOMBT would become equal to 20491 years.)

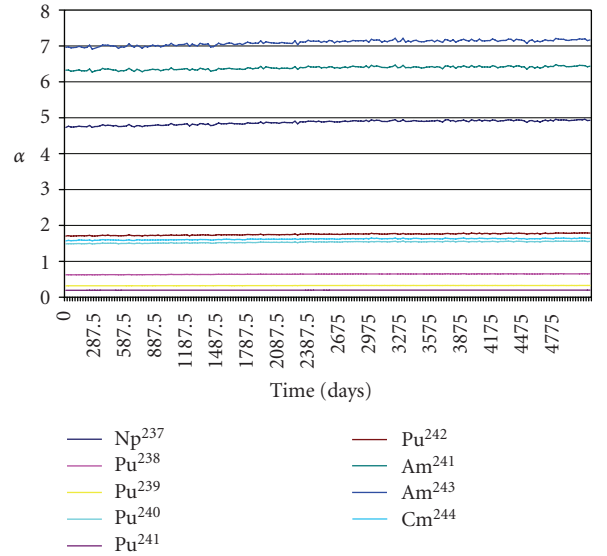

Figure 11: α versus time in GCFR (fluctuations are due to the MC method adopted in our calculations).

Table 10: 1-group α ratio at BOC.

	GCFR	PBMR
U^{238}	5.27	—
Np^{237}	4.73	200
Pu^{238}	0.62	14.25
Pu^{239}	0.32	0.60
Pu^{240}	1.49	416.67
Pu^{241}	0.19	0.36
Pu^{242}	1.70	204.08
Am^{241}	6.33	119.05
Am^{243}	6.96	333.33
Cm^{244}	1.57	30.96

5.3.3. *Discussion on the obtained results*

As figure of merit, we have considered the α ratio, $\alpha = \sigma_c/\sigma_f$. This ratio value versus burnup remains substantially constant or suffer limited variations that can be neglected (e.g., see Figure 11). This justifies our choice to assume the value of α at BOC valid for the whole irradiation time.

It is possible to highlight the fact that the higher the α ratio, the higher the probability of capture than fission for the considered nuclide in the given flux.

From Table 10, we can analyze the results we have obtained.

The capture-to-fission ratio comes in fact from the effective cross-sections. These last have obtained weighting over the neutron spectrum, as we have seen in the first part of this paper. In fast reactors, the neutron spectrum is less dependent from variations of the fuel composition than in

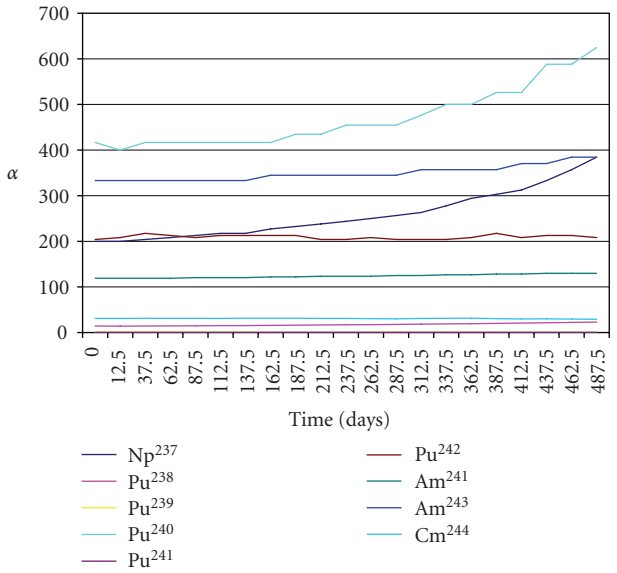

Figure 12: σ_a versus E of some HMs (Pu^{239} in red color, Pu^{240} in green, Pu^{241} in blue, Pu^{242} in purple, Am^{241} in light green) [35].

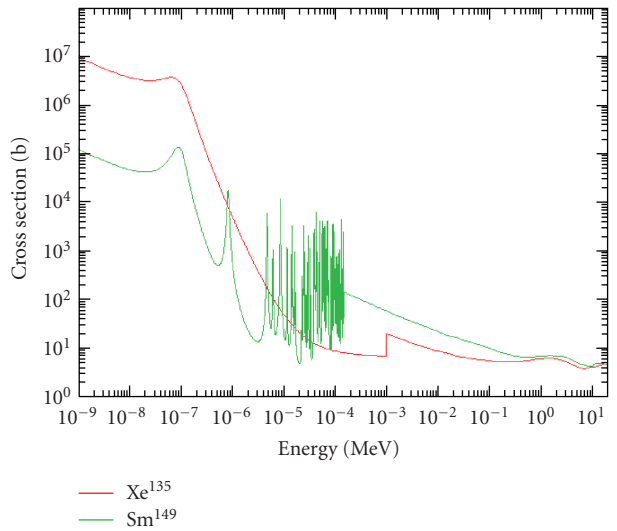

Figure 13: σ_a versus E of some FPs (Xe^{135} in red color, Sm^{149} in green) [35].

thermal reactors. In fact, during burnup FPs and actinides with higher mass number buildup. FPs have generally a high-capture cross-section in thermal and/or epithermal range, while the HM with higher mass number has often larger absorption cross-sections in this same energy range than the actinides more abundant in the fresh fuel (i.e., U^{238} and Pu^{239}) [35], Figures 12 and 13, so that at EOC in thermal reactors the spectrum becomes harder, because its softer tail is absorbed by these nuclides.

This effect is negligible in fast spectrum, so that we obtain the trend shown in Figure 11.

Concerning the Pu fissile isotopes (i.e., Pu^{239} and Pu^{241}), they burn better in fast spectrum than in thermal one. (α in fast spectrum is lower than in thermal for both,

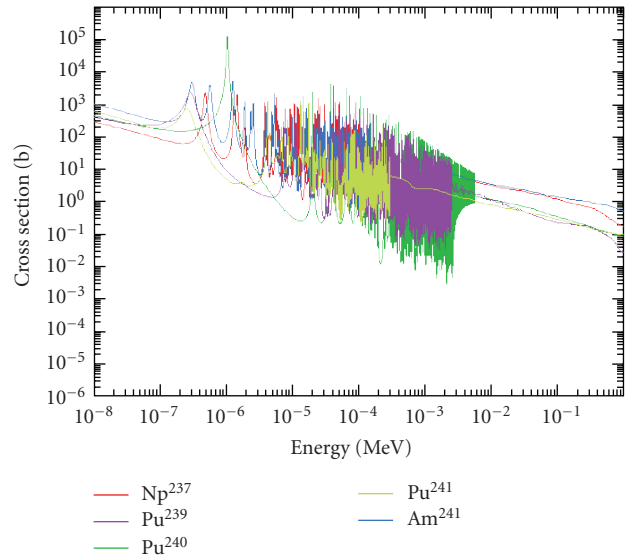

Figure 14: Comparison of the absorption cross-sections among some nuclides (Np^{237} in red, Pu^{239} in purple, Pu^{240} in green, Pu^{241} in light green, Am^{241} in blue) [35].

Table 11: Property data of some fuel compound [5].

	$UPuO_2$	UPuC	UPuN
Density [g/cm^3]	11.0	13.6	14.3
HM density [g/cm^3]	9.7	12.9	13.5
T_{melt} [°C]	2775	2480	2780
Thermal conductivity [W/mK]	2.9	19.6	19.8

the probability of fission is higher than that of capture.) Particularly, in the PBMR the quantity of Pu^{239} decreases of about 20%, while its daughter Pu^{240} is also slightly reduced despite its high α ratio ($\approx$417): this is due to Pu^{239} transmutation by capture. Please note also that there is not a production channel of Pu^{239} because the fuel is fertile-free. In PBMR, Pu^{241} also slightly decreases and transmutes partially in Pu^{242} that builds up during irradiation. In GCFR, α of these nuclides is smaller than in PBMR: in fact there is a higher probability to have fission. Their daughters Pu^{240} and Pu^{242} are both decreasing. Nevertheless, the total amount of Pu^{239} multiplies in GCFR by a factor three during burnup because of the behavior of its parent U^{238}. This fact is positive in order to obtain an effective self-sustaining core with a full-actinide recycle. In fact, if the Pu isotopic vector would be too much degraded, the criticality would be probably not maintained in the following cycle substituting the FPs only with pure DU.

Concerning the chain $Np^{237} \rightarrow Pu^{238}$, Np^{237} has a high α both in thermal and fast spectrum: its transmute in Pu^{238} by capture. Obviously, the quantity of Np^{237} that transmutes in GCFR is higher because in thermal spectrum, it has to compete with other strong absorbers (Figure 14). In this GCFR core, Pu^{238} is fissile and its quantity decreases during irradiation.

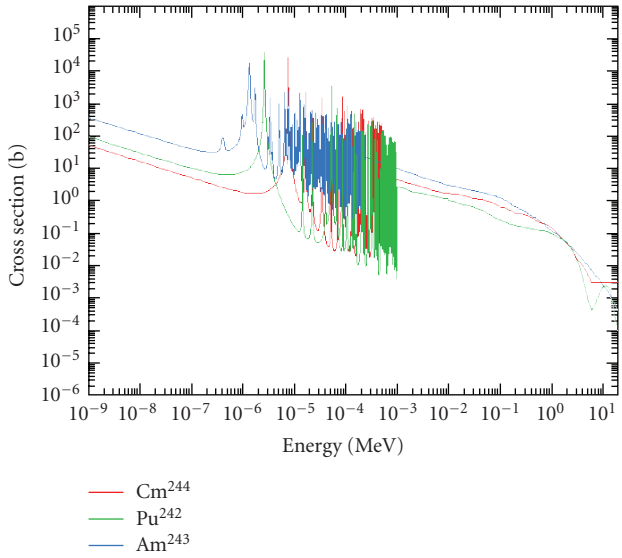

Figure 15: Comparison among some absorption cross-sections (Cm^{244} in red, Pu^{242} in green, Am^{243} in blue) [35].

Regarding the chain of Cm^{244} that at the moment is the most difficult nuclide to be burnt, we can observe the following.

(1) In the thermal spectrum, Cm^{244} grows a lot. In fact, its precursors (Pu^{242} and Am^{243}) both increase and have a large α ratio (resp., 204 and 333). Moreover, Cm^{244} has a very low absorption cross-section, if compared with the other nuclides in the fuel (Figure 15).

(2) In the fast spectrum, Cm^{244} has a lower growing rate, because Pu^{242} and Am^{243} are both decreasing, and the absorption cross-sections of the HMs are all comparable in this range. Moreover, α is not too large for all these nuclides.

Finally, there is something more related to Am^{241}: the thermal spectrum burns it very good thanks to its high capture cross-section (Figures 12 and 14); while in GCFR, the amount of this nuclide has a nonmonotonic trend (Figure 16). Its main production channel is the β^- decay of Pu^{241} (half-life = 14.4 years). The total irradiation time is comparable (4950 days) with the Pu^{241} half-life (14.4 years are about 5250 days). On the other hand, the most part of Pu^{241} is transmuted by absorption. The production of Am^{241} can be expressed in a simplified manner as

$$\frac{d\mathrm{Am}^{241}}{dt} = \lambda^{\mathrm{Pu}^{241}} \cdot \mathrm{Pu}^{241} - \sigma_a^{\mathrm{Am}^{241}} \cdot \varphi \cdot \mathrm{Am}^{241}, \qquad (24)$$

where Am^{241} and Pu^{241} are the time-dependent quantities of the considered nuclides. ($\lambda^{Pu^{241}}$) and ($\sigma_a^{Am^{241}} \cdot \varphi$) are, respectively, $1.53 \cdot 10^{-9}\,s^{-1}$ and $3.2 \cdot 10^{-9}\,s^{-1}$. Now, we can do some qualitative considerations. At beginning and for the most part of the cycle, the first term of the right hand of this equation makes the exponential solution increasing

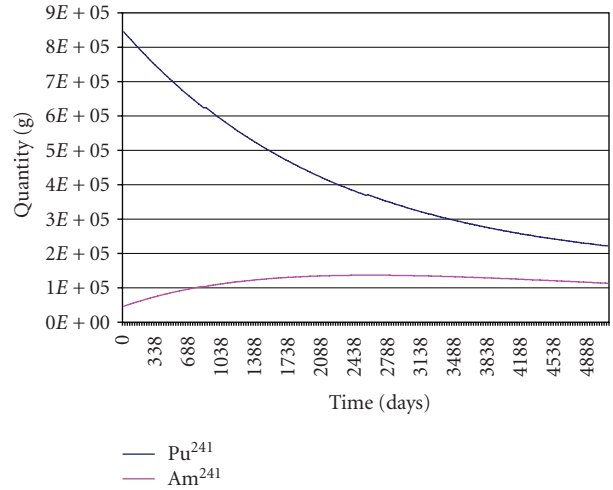

Figure 16: Quantity versus time of Pu^{241} and Am^{241}.

because of the relatively high Pu^{241} initial quantity. The solution of the equation reaches a maximum, and then it starts to decrease, because the quantity of Am^{241} is not more negligible (the product $\sigma_a^{Am^{241}} \cdot \varphi$ has no significant changes due to the fast spectrum), see also Figure 16.

6. CONCLUSIONS AND FUTURE PERSPECTIVES

This work represents a contribute to the researches on the important topic of waste reduction. In fact, from the results we can see that HTRs reduce waste radiotoxicity of an order of magnitude burning Pu and supplying energy. Adopting Th-Pu-based cycle, it appears that the total amount of produced energy is quite large.

The use of GCFR after HTR fuelled with Pu-U (or Pu-Th) is capable to further reduce radiotoxicity in the waste and gives back (as expected) almost the same amount of Pu initially loaded and, at the same time, supplies a lot of energy. It is important to underline that this Pu, used as fuel, is not a waste but a source of energy, not a problem but a resource [36]. It is important to highlight the progress in this research performed in the last period. In fact, while in our first papers [14, 20, 30] on this topic, the calculations were performed on simplified models (k_{inf}, etc.), the most recent calculations (reported in the final part of this paper) were performed on a "real" model of the studied reactors (both PBMR and GCFR). In addition, we have added the GCFR multiple recycling option using k_{eff} calculations for all the considered reactors.

Regarding the future perspectives, the material technology is probably the most challenging aspects in innovative reactor and fuel cycles field. In fact, the fuel has to be stable under high temperature and high fast fluence, simply to be reprocessed and refabricated. Moreover, it has also to contain a consistent fraction of MA, which has often a chemical behavior different not only from U but also from Pu. Moreover, their extensive use as fuels will require additional shielding respect to the actual reprocessing and fabrication

plants: many MAs are so strong γ and neutrons emitters that it is impossible to adopt the actual MOX fabrication technology to treat them.

Carbide and nitride are very interesting chemical forms for the new fuel concepts: they have a larger thermal conductivity and a higher density of HM than oxides (Table 11) but many technological studies have to be still performed on this topic. (The higher HM density allows to obtain criticality also with higher volumetric fraction of coolant in the core. This fact is very important for GCFR design [5].)

Recovering of all the HMs from SNF is another aspect to be investigated. For instance, for the *integral fuel cycle* proposed for GCFR, all the HMs have to be together extracted during reprocessing and then used to manufacture new fuel. It is clear that to find an extracting molecule (or a group of molecules) that allows the selective extraction of all the actinide together is a complex issue. Other problems are partitioning of actinides (especially the trivalent ones) from lanthanides and Am from Cm [37, 38].

At the end of the proposed symbiotic cycle, the waste results to be virtually made up only by fission products, that was be separated by the actinides, whose best repository seems to be the new GCFR core itself, in order to further reduce the HLW and best exploit the uranium resources.

Moreover, the LOMBT is reduced to less than 200 years. Please remember that in an LWR, using a *once-through* cycle (even if a MOX technology is adopted), the LOMBT will be reached after more than 100000 years.

It is important also to highlight that we adopt, in proposed recycling scheme, only chemical and not isotopic separations: in this way, it is possible to reduce the costs and to avoid proliferation concerns linked to the use of plutonium.

Finally, we can underline that GCFR is a "real" reactor not a simple burner that, while burning MA, produces energy. Furthermore, considering the positive characteristics of HTR in terms of Pu burning due to their excellent neutronic economy, and coupling it with GCFR (fast neutronic spectrum and high fluence) in a symbiotic fuel cycle, we can say that the geological disposal issues concerning high level radiotoxicity of actinides can be considerably reduced.

ABBREVIATIONS

An: Actinides
BG: Breeding gain
BWR: Boiling water reactor
CP: Coated particle
DU: Depleted uranium
EFPD: Effective full power days
FIMA: Fission per initial metal atom
FP: Fission products
GCFR: Gas cooled fast reactor
HM: Heavy metal (actinides)
HTR: High temperature reactor
LFR: Lead-cooled fast reactor
LMFBR: Liquid metal fast breeder reactor
Ln: Lanthanides
LOM: Level of mine
LOMBT: Level of mine balancing time
LWR: Light water reactor
MA: Minor actinides
MC: Monte carlo
MOX: Mixed oxide
MSR: Molten salt reactor
OTTO: Once through then out
PWR: Pressurized water reactor
RG: Reactor grade
SCWR: Super-critical water-cooled reactor
SFR: Sodium-cooled fast reactor
SNF: Spent nuclear fuel
STP: Standard temperature and pressure
TRU: TRans-Uranics
VHTR: Very high temperature reactor
WG: Weapons grade.

ACKNOWLEDGMENTS

The work presented in this paper was partly funded by the European Union Sixth Framework Program, under contracts GCFR, PuMA, and RAPHAEL. First of all, we like to thank Dr. Kuijper and Dr. van Heek both of NRG, Professor Kloosterman of TUD, Dr. von Lensa of FZJ, and Dr. Mitchell of AMEC-NNC for their support. Finally, we want to thank Professor G. Forasassi of DIMNP for his very appreciated collaboration and Dr. D. Bufalino of DIMNP for his precious suggestions and help.

REFERENCES

[1] E. E. Bende, *Plutonium burning in a pebble-bed type high temperature nuclear reactor*, Ph.D. thesis, Delft University of Technology, Delft, The Netherlands, 1999.
[2] http://world-nuclear.org/.
[3] IAEA, "Implications of partitioning and transmutation in radioactive waste management," Tech. Rep. 435, IAEA, Vienna, Austria, 2004.
[4] U.S. DOE Nuclear Energy Research Advisory Committee and the Generation IV International Forum, "A technology roadmap for generation IV nuclear energy systems," December 2002.
[5] W. F. G. van Rooijen, *Improving fuel cycle design and safety characteristics of a gas cooled fast reactor*, Ph.D. thesis, Delft University of Technology, Delft, The Netherlands, 2006.
[6] OECD/IAEA, *Uranium 2005: Resources, Production and Demand*, NEA and IAEA, Paris, France, 2006.
[7] H. W. Wiese, "Actinide transmutation properties of thermal and fast fission reactors including multiple recycling," *Journal of Alloys and Compounds*, vol. 271–273, pp. 522–529, 1998.
[8] N. Cerullo, *Lezioni di Ingegneria del nocciolo*, DIMNP, Pisa, Italy, 1988.
[9] T. Iwasaki and N. Hirakawa, "Fast and perfect transmutation of actinide wastes using A-Burner," in *Proceedings of the International Conference on Future Nuclear Systems: Emerging Fuel Cycles and Waste Disposal Options*, pp. 622–629, Seattle, Wash, USA, September 1993.
[10] G. Lomonaco, *I recenti sviluppi dei reattori a gas ad alta temperatura. La collocazione di questi impianti nel futuro piano energetico mondiale. Il programma europeo HTR-N e l'attività di ricerca del DIMNP svolta nel suo ambito*, M.S. thesis, University

of Pisa, Pisa, Italy, June 2003, http://www.tesionline.it/default/tesi.asp?idt=10251.

[11] E. Bomboni, *Le scorie nucleari: analisi della loro possibile riduzione mediante cicli di combustibile innovativi*, M.S. thesis, University of Pisa, Pisa, Italy, July 2006, http://etd.adm.unipi.it/theses/available/etd-06122006-143839/.

[12] T. D. Newton and P. J. Smith, "A moderated target subassembly design for minor actinide transmutation," in *Proceedings of the Global 2003: Atoms for Prosperity: Updating Eisenhower's Global Vision for Nuclear Energy*, pp. 1028–1037, New Orleans, La, USA, November 2003.

[13] D. C. Wade, "Safety considerations in design of fast spectrum ADS for transuranic and minor actinide burning: a status report on activities of the OECD-NEA expert group," in *Proceedings of the 6th Information Exchange Meeting on Actinide and Fission Product Partitioning and Transmutation*, Madrid, Spain, December 2000.

[14] N. Cerullo, D. Bufalino, G. Forasassi, G. Lomonaco, P. Rocchi, and V. Romanello, "The capabilities of HTRs to burn actinides and to optimize plutonium exploitation," in *Proceedings of the 12th International Conference on Nuclear Engineering (ICONE '04)*, vol. 1, pp. 495–501, Arlington, Va, USA, April 2004.

[15] http://www.cea.fr/.

[16] J. F. Briesmeister, Ed., "MCNP—a general Monte Carlo code N-particle transport code, version 4B," LANL report LA-12625-M, Los Alamos National Laboratory, Los Alamos, NM, USA, March 1997.

[17] O.R.N.L., "ORIGEN 2.1 isotope generation and depletion code matrix exponential method," Tech. Rep. CCC-371, Oak Ridge National Laboratory, Radiation Safety Information Computational Center, Oak Ridge, Tenn, USA, August 1996.

[18] http://www.nea.fr/.

[19] V. Romanello, *Analisi di alcune peculiari potenzialità degli HTR: la produzione di idrogeno ed il bruciamento degli attinidi*, M.S. thesis, University of Pisa, Pisa, Italy, October 2003, http://etd.adm.unipi.it/theses/available/etd-10152003-181233/.

[20] N. Cerullo, D. Bufalino, G. Forasassi, G. Lomonaco, P. Rocchi, and V. Romanello, "An additional performance of HTRs: the waste radiotoxicity minimization," *Radiaction Protection Dosimetry*, vol. 115, no. 1–4, pp. 122–125, 2005.

[21] D. I. Poston and H. R. Trellue, "User's manual, version 2.0 for MONTEBURNS version 1.0," Tech. Rep. LA-UR-99-4999 PSR-0455/01, Los Alamos National Laboratory, Los Alamos, NM, USA, September 1999.

[22] http://www.perl.com/.

[23] L.A.N.L., "MCNPX, version 2.6c," November 2006.

[24] J. Cetnar, W. Gudowski, and J. Wallenius, "User manual for Monte-Carlo continuous energy burnup (MCB) code—version 1C," http://www.nea.fr/abs/html/nea-1643.html.

[25] J. Cetnar, "A method of transmutation trajectories analysis in accelerator driven system," in *Proceedings of IAEA Technical Committee Meeting on Feasibility and Motivation for Hybrid Concepts for Nuclear Energy Generation and Transmutation*, Madrid, Spain, September 1997.

[26] ANSWER Software Service, "WIMS-D/5: a neutronic code for standard lattice physics analysis," A.E.A. Winfrith, 1995.

[27] N. M. Greene and L. M. Petrie, "XSDRNPM: a one-dimensional discrete-ordinates code for transport analysis," Tech. Rep., Oak Ridge National Laboratory, Oak Ridge, NM, USA, March 2000.

[28] V. Romanello, G. Lomonaco, and N. Cerullo, "CARL 2.2 code's user manual," http://www.nea.fr/abs/html/nea-1735.html.

[29] J. C. Kuijper, X. Raepsaet, J. B. M. de Haas, et al., "HTGR reactor physics and fuel cycle studies," *Nuclear Engineering and Design*, vol. 236, no. 5-6, pp. 615–634, 2006.

[30] N. Cerullo, G. Lomonaco, and V. Romanello, "Waste radiotoxicity minimization using innovative LWR-HTR-GCFR symbiotic fuel cycles," in *Proceedings of the Workshop on Advanced Reactors with Innovative Fuels (ARWIF '05)*, Oak Ridge, Tenn, USA, February 2005.

[31] T. A. Taiwo, T. Y. C. Wei, E. E. Feldman, et al., "Particle-bed gas-cooled fast reactor (PB-GCFR) design," Tech. Rep. NERI 01-022, Argonne National Lab, Argonne, Ill, USA, September 2003.

[32] A. Conti and J. C. Bosq, "600 MWth GFR cores containing plates CERCER—characteristics," CEA-Cadarache, France, December 2004.

[33] http://www.gcfr.org/.

[34] E. Bomboni, N. Cerullo, G. Lomonaco, and V. Romanello, "Nuclear waste impact reduction using multiple fuel recycling strategies," in *Proceedings of the 1st International Conference on Physics and Technology of Reactors and Applications (PHYTRA '07)*, Marrakech, Morocco, March 2007.

[35] MCNP Libraries from ENDF/B-6.x, http://atom.kaeri.re.kr/.

[36] S. Massara, P. Tetart, and L. Boucher, "A French scenario for fast reactors deployment over the XXIst century," in *Proceedings of the Workshop on Advanced Reactors with Innovative Fuels (ARWIF '05)*, Oak Ridge, Tenn, USA, February 2005.

[37] J. M. Adnet, M. Miguirditchian, C. Hill, et al., "Development of new hydrometallurgical processes for actinide recovery: GANEX concept," in *Proceedings of International Conference on Nuclear Energy Systems for Future Generation and Global Sustainablity (Global '05)*, Tsukuba, Japan, October 2005.

[38] OECD/NEA, "Actinide separation chemistry in nuclear waste streams and materials," Tech. Rep. NEA/NSC/DOC(97)19, Organisation for Economic Co-operation and Development, Paris, France, December 1997.